Accepted Manuscript

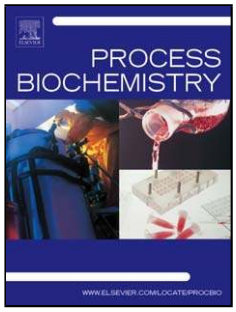

Title: Reactive Oxygen Species Mediated Modifications in *Bacillus subtilis* Lipid Membrane to Improve Protein Productivities

Authors: Harit Mohan, K. Uma Maheswari, Amal K. Bera, G.K. Suraishkumar

PII: S1359-5113(09)00344-4
DOI: doi:10.1016/j.procbio.2009.11.003
Reference: PRBI 8780

To appear in: *Process Biochemistry*

Received date: 19-5-2009
Revised date: 2-11-2009
Accepted date: 4-11-2009

Please cite this article as: Mohan H, Maheswari KU, Bera AK, Suraishkumar GK, Reactive Oxygen Species Mediated Modifications in *Bacillus subtilis* Lipid Membrane to Improve Protein Productivities, *Process Biochemistry* (2008), doi:10.1016/j.procbio.2009.11.003

This is a PDF file of an unedited manuscript that has been accepted for publication. As a service to our customers we are providing this early version of the manuscript. The manuscript will undergo copyediting, typesetting, and review of the resulting proof before it is published in its final form. Please note that during the production process errors may be discovered which could affect the content, and all legal disclaimers that apply to the journal pertain.

*Manuscript
ACCEPTED MANUSCRIPT

Reactive Oxygen Species Mediated Modifications in *Bacillus subtilis* Lipid Membrane to Improve Protein Productivities

Harit Mohan[1], K. Uma Maheswari[2], Amal K. Bera[1], and G.K. Suraishkumar[1,]*
[1] Department of Biotechnology, Indian Institute of Technology Madras, Chennai 600036 INDIA
[2] School of Chemical and Biotechnology, SASTRA University, Thanjavur 613402, INDIA

Running title: ROS effects on *B. subtilis* Lipid Membrane

Keywords: oxidative stress; reactive oxygen species; bilayer lipid membrane; lipid peroxidation; amylase; protease

* Author for correspondence:
G. K. Suraishkumar
Department of Biotechnology, Bhupat and Jyoti Mehta School of Biosciences building,
Indian Institute of Technology Madras, Chennai 600 036 INDIA
Phone: +91 44 2257 4105
Fax: +91 44 2257 4102
Email: gk@iitm.ac.in

Accepted Manuscript

ACCEPTED MANUSCRIPT

Abstract

The overall objective of this work was to investigate the modifications that occur in *Bacillus subtilis* lipid membrane during induced oxidative stress caused by reactive oxygen species (ROS), via an electrophysiological approach. Further, based on the results, we have developed and demonstrated a novel strategy to enhance specific enzyme production. Electrical parameters such as phase angle (θ), impedance (Z), capacitance (C) and breakdown voltage of reconstituted bilayer lipid membrane (BLM) composed of lipids extracted from non-stressed, mildly stressed (2.5 mM H_2O_2) and strongly stressed (2.5 mM H_2O_2 with 100 μM $FeSO_4$) *B. subtilis* were compared. Strongly stressed BLM showed lower values of θ (10°), Z (0.4 Mohm), and breakdown voltage (100 mV) in comparison with those observed for non-stressed BLM, i.e. 30°, 0.5 Mohm and 250 mV, respectively. The capacitance of strongly stressed BLM, however, was higher (2.28 nF) compared to that of the non-stressed BLM (0.4 nF). These results suggest that under strongly stressed conditions, the lipids were loosely packed that resulted in a more permeable BLM. The higher permeability seems to result, unexpectedly, from a higher unsaturated fatty acid (UFA) synthesis and membrane incorporation (UFA fraction increased by 227%), and expectedly, from increased lipid peroxidation (increased by nearly 200%) in the BLM. A strategy that is based on increased membrane permeability due to induced ROS, enhanced specific amylase and protease production under oxidative stress by 62% and 137%, respectively.

Accepted Manuscript

ACCEPTED MANUSCRIPT

Introduction

The cell membrane acts as a selective permeable barrier, and the hydrophobic chains of lipids disallow transport of polar solutes and ions across it [1]. The cell can regulate its membrane permeability through a change in its lipid composition [2]. Also, the lipid composition of the membrane is significantly determined by the environmental conditions of the cell [3, 4]. For example, when *Bacillus subtilis* cells were subjected to low temperature, an increased incorporation of unsaturated fatty acids (UFA) and decreased incorporation of saturated straight chain was observed [5, 6]. The UFA have lower melting points compared to their saturated counterparts, and hence the membrane fluidity is maintained during cold shock [7]. Similar changes in lipid composition when cells were subjected to salt, thermal, or acid stress have also been reported [5]. The effect of oxidative stress, however, and more specifically, the effect of reactive oxygen species (ROS) on *B. subtilis* cell membrane composition and properties have not been reported.

Oxidative stress is caused by the family of ROS that predominantly includes superoxide ion, hydroxyl free radical and hydrogen peroxide [8]. Addition of hydrogen peroxide, a weak inducer of oxidative stress, to the medium can be used to deliberately induce hydroxyl radical formation in bacteria to study cellular response [9]. To cause a more severe stress through higher concentration of hydroxyl radicals, $FeSO_4$ can be supplemented in growth media; the Fe^{2+} present in media quickly reacts with H_2O_2 to produce hydroxyl radical by Fenton's reaction [10]. The overwhelming production rate of hydroxyl radical from H_2O_2 is unmatched to the increase in the rate of H_2O_2 quenching by catalase and glutathione peroxidase, which leads to induced oxidative stress [11, 12].

ACCEPTED MANUSCRIPT

The hydroxyl radical is the most deleterious ROS, and it damages bases of DNA, leads to protein carbonylation and lipid peroxidation [13, 14]. The UFA in membrane lipids are highly susceptible to damage by the hydroxyl radicals. They undergo lipid peroxidation wherein carbonyl compounds such as malondialdehyde (MDA) and 4-Hydroxy alkenals (HNE) are formed as byproducts. The amount of MDA formed has been used as an oxidative stress index [15].

Bimolecular/bilayer lipid membrane (BLM) has been used to study changes in cellular membrane permittivity, permeability and transport across bilayer [16] during oxidative stress. BLM is known to behave as an electrical capacitor and exhibits electrical properties such as impedance, resistance, capacitance, etc., [17].

An electrophysiological approach to study the changes in the electrical properties of the BLM formed from the lipids isolated from non-stressed and oxidative stressed *B. subtilis* cells have been used for the first time to infer the modifications that occur in *B. subtilis* cellular lipid bilayer during oxidative stress conditions. Several electrical parameters of the *B. subtilis* BLM that will be helpful in mathematical modeling and electrophysiological studies have been determined in this work. The changes in lipid peroxidation and the UFA fraction have been investigated to understand the effect of oxidative stress on the BLMs. From the results, the unsaturated fatty acids present in the form of phospholipid in *B. subtilis* cell membrane, during non-stressed and oxidative stress conditions have also been estimated. In addition, a novel strategy to improve specific amylase and protease productivity by *B. subtilis* through oxidative stress has been demonstrated.

ACCEPTED MANUSCRIPT

Materials and methods

Bacterial strain and growth conditions. *B. subtilis* 168 was grown in bioreactor (Bioengineering AG, Switzerland) to a final volume of 2 l in 2.5% Luria Bertani (LB, Miler, Himedia, India) medium. For all experiments the reactor conditions were pH 7.0, 30% dissolved oxygen and 37 °C temperature. The culture was harvested at the late log phase to achieve maximum cell yield for lipid isolation and to avoid cells from undergoing nutrient starvation or other stationary phase stresses.

Oxidative stress induction procedure. The cells were exposed to two levels of oxidative stresses in different experiments. To induce a mild oxidative stress condition (referred to as mild stress in this manuscript), 2.5 mM H_2O_2 was added to the culture at 30 min intervals until onset of stationary phase. To induce a comparatively stronger but non-lethal stress (referred to as strong stress in this manuscript), 100 μM $FeSO_4$ was added to medium just before inoculation and H_2O_2 was added every 30 min as above. No H_2O_2 was added to the control culture.

Lipid isolation. For all three kinds of samples, the culture at late log phase was harvested by centrifugation at 12,000g for 10 min to pellet down the cells, followed by wash with saline (0.9% NaCl). The cells were used for lipid isolation and supernatant was collected to perform other assays. The lipid isolation procedure reported by Bligh and Dyer (1959) was used, in principle [18]. Briefly, for every 1 g of cell 8 ml saline, 20 ml chloroform (SRL, India) and 26 ml methanol (SRL, India) was added. 1 M sodium acetate buffer (pH 4.0) was added to a final concentration of 0.1 M. For the extraction of lipids the mixture was shook for 2 h. The lower chloroform layer was separated carefully using a separating funnel. The samples were concentrated by purging nitrogen gas to

Accepted Manuscript

ACCEPTED MANUSCRIPT

evaporate chloroform and the extracted lipid samples were preserved in N_2 environment at -40°C. To confirm the quality of lipids, thin layer chromatography (TLC) [19] with chloroform:methanol (25:25) as the mobile phase and phosphate stain was used.

Bilayer formation. 4% (w/v) dispersion of lipids in n-decane for all three kinds of lipids was prepared after completely evaporating chloroform using N_2 gas. Both *cis* and *trans* compartments of polymethylmethacrylate (PMMA) chamber (custom made) were filled with 3.5 ml of bath solution (HEPES buffer pH 7.0, 0.05 M KCl). Salt bridge and Ag/AgCl electrodes were used for electrical contacts. 5 µl of lipid dispersion was applied by micropipette to aperture (area 0.00705 cm^2) and left for 30 min for stabilization. BLM formation was monitored by following membrane capacitance (in AC studies) and current (in DC studies).

Determination of BLM electrical properties. The electrical properties of the BLM, namely capacitance (C), resistance (R), impedance (Z) and theta (θ) were determined using frequency dependent dispersion (at constant voltage of 40 mV) and voltage dispersion (at constant frequency of 100 Hz). The LCR meter (Chroma 1062A, Chroma Ate Inc**.,** Taiwan) was used for the dispersion studies. The voltage and frequency was increased in steps every 3 min to observe change in BLM properties.

To determine the various relevant BLM parameters, namely, the constants A', λ, time constant, τ, leakage current, DC capacitance and relative permittivity, ε, the membrane currents at different applied DC source voltages (40-150 mV) were investigated using Keithley 6514 electrometer (Keithley Instruments Inc., Ohio). In the circuit that was set up, the BLM was in series with 1 Gohm resistor and an ammeter. Charging and discharging of BLM was done by connecting and disconnecting the

ACCEPTED MANUSCRIPT

variable DC supply respectively. Data acquisition was done using computer interfacing software (Exelinx) that recorded current across BLM at a frequency of 2.59 Hz. Generated data was processed using MS Excel 2003 and MATLAB 7.0. Curve fitting, equation parameters estimation and charge vs. time graph were made using standard MATLAB command lines.

Lipid peroxidation estimation: MDA assay. A standard MDA assay procedure [20] was followed, in principle, and the details are as follows. Lipids, 0.15 ml, dissolved in chloroform were vacuum-dried and weighed before the assay. Chilled tri-chloro acetic acid (TCA) (10% w/v), 0.1 ml, was added to the isolated lipid sample and kept on ice for 15 min to get a de-proteinized membrane sample. Contents were centrifuged at 12,000g for 10 min, and to the supernatant, 0.2 ml of thiobarbituric acid, TBA (Himedia, India) (67 mg TBA in 1 ml DMSO and 9 ml of water) was added and heated for 30 min at 95 °C. To estimate the protein "bound" MDA, 0.2 ml culture supernatant was processed as above with a few modifications. The modifications: after TCA addition the sample was centrifuged, 0.35 ml of TBA was added to the supernatant and kept at 95 °C for 15 min. OD at 532 nm was used to determine specific MDA level in lipids, and in the supernatant. The standard curve was prepared using 1,1,3,3- tetramethoxypropane (Himedia, India) [21].

UFA fraction estimation: Iodine number. Isolated lipids were diluted in 2 ml of chloroform such that final concentration was 2-3 mg ml^{-1}. 3 ml of pyridine sulfate dibromide solution was added and incubated for 15 min at 25 °C. After addition of 0.5 ml of KI (10%) final solution was titrated with 0.02 N $Na_2S_2O_3$. By using the standard relation that 1 ml of 0.1 M sodium thiosulphate solution = 0.01269 g of iodine. Iodine

ACCEPTED MANUSCRIPT

number is given by following formula where *a* is blank titration volume, *b* is volume of 0.02 N $Na_2S_2O_3$ consumed and *c* is weight of phospholipid sample in g [22].

$$\frac{a-b}{c} X \frac{1.27}{2} = Iodinenumber$$

Protease estimation. Protease estimation was done as reported earlier [9]. Briefly, to 0.5 ml of supernatant 0.2 ml of azocasein (sigma) solution was added and incubated for 1 h at 37°C. The reaction was stopped by addition of 0.3 ml of TCA (10% w/v) and samples were then centrifuged at 15,000g for 5 min. 0.8 ml of supernatant from each tube was transferred to another glass tube and 0.4 ml NaOH (2 M) was added. The contents were mixed and absorbance was monitored at 440 nm against a blank. Standard curve was plotted using known amount of trypsin (Sigma).

Amylase estimation. 50 µl of supernatant was added to 0.25 ml of starch (SRL, India) (1% w/v) and incubated for 1 h at 50 °C. The reducing sugars formed were determined by adding 0.5 ml of 3, 5-dinitrosalicylic acid (DNS) and heating at 90°C for 15 min. OD at 540 nm was determined and one unit of α-amylase is defined as the amount of enzyme required to produce 1 µM of reducing equivalents per minute from soluble starch under the assay conditions. The standard curve was made using glucose[23].

Accepted Manuscript

ACCEPTED MANUSCRIPT

Results and Discussion

Oxidative stress modifies the electrical properties of *B. subtilis* BLM

To understand the effects of oxidative stress on the *B. subtilis* lipid membrane, the isolated lipids from non-stressed, mildly- and strongly- stressed cells were reconstituted to form BLMs. The BLM acts as a capacitor with the hydrocarbon chains as the dielectric and the polar head groups as charged plates [24]. Four different electrical parameters for non-stressed, mildly- and strongly- stressed BLMs, such as phase angle (θ), impedance (Z), capacitance (C) and breakdown voltage were compared to understand the possible modifications in the membrane structure and composition that occur during oxidative stress.

The value of the phase angle (θ), between the voltage, V, and the current, I, of the capacitor [25], indicates the ability of the BLM capacitor to prevent passage of current through it. In standard representation, $V = V_0 \sin(\omega t)$, and $I = I_0 \sin(\omega t + \theta)$, where V_0 is the maximum voltage, I_0 is the maximum current, ω is the angular frequency of AC voltage, and t is time. Saturated chains of lipids pack well in a BLM due to their straight-chain geometries; the well stacked lipids improve the dielectric nature of the BLM [26], and disallow charge leakage, which result in a larger phase angle. On the other hand, the unsaturated or branched chains of lipids or short chained lipids pack loosely in a BLM [27]; the loose packing facilitates charge leakage across the BLM, reduces its dielectric nature, and thus results in smaller phase angle values and higher currents.

The BLM formed from non-stressed *B. subtilis* lipids (non-stressed BLM) was found to possess a phase angle (θ) of nearly 30° at 40 mV and 100 Hz after 2 h. The relatively

ACCEPTED MANUSCRIPT

low θ value of non-stressed BLM may be due to branched chain fatty acids (iso and anteiso) that are predominantly present (~95%) in *B. subtilis* membrane [19]. The θ values for mildly and strongly stressed samples were found to be even lower at 15° and 10° respectively under similar conditions. Physiologically, the θ value signifies disorder in the arrangement of lipids in cell membrane. Our results suggest that the strongly stressed BLM has maximum disorder in lipids packing followed by mildly stressed BLM. Further, non-stressed BLM which has highest phase angle amongst the three BLMs, has the most efficient packing. The lower leakage current in the non-stressed BLM (Table 1) also implies better packing efficiency of lipids.

The impedance (*Z*), typically a representation of the opposition to current in an AC circuit, is used here as a measure of the overall resistance of the passage of current across the BLM. The higher values of impedance, *Z* may be due to the presence of well stacked lipids, which act as an insulator (dielectric) between the conducting, buffer-filled, *cis* and *trans* aqueous compartments (plates of capacitor) [28]. Voltage dispersion, in which the voltage was increased in steps with time and frequency of AC current was kept constant; and frequency dispersion, in which the frequency was increased in steps with time and voltage of AC current was kept constant, were used to study impedance of non-stressed, mildly stressed, and strongly stressed BLMs. The increase in applied voltage during voltage dispersion studies is known to increase the distribution of ions at BLM-bulk interface, which in turn, leads to membrane perturbation. Such perturbations cause the formation of small breaches and defects in the BLM, which may provide passage for the conduction of ions, and thus, result in decreased impedance [24].

ACCEPTED MANUSCRIPT

We observed a constant decrease in impedance with increasing voltage and frequency in the case of voltage and frequency dispersion studies respectively (Figure 1). In voltage dispersion studies with non-stressed BLM, a decrease in impedance from 3.73 Mohm at 40 mV to 0.24 Mohm at 250 mV, implies a proportionate increase in conductance of charges across the BLM (Figure 1a). At 150 mV, the non-stressed BLM and the mildly stressed BLM have nearly the same impedance of about 0.5 Mohm, which was found to be higher than the impedance of strongly stressed BLM (0.4 Mohm). In the case of frequency dependent dispersion of impedance shown in Figure 1b (Bode plot), it is observed that there is a decrease in impedance values for all three types of BLMs (non-stress, mildly stressed and strongly stressed) with increasing frequency. This is typical of a capacitive circuit. At low frequencies, a capacitor blocks the current while at high frequencies, current is free to flow through the capacitor and the limiting parameter is the resistance. However, it is noticed that the decrease in impedance for the mildly stressed and strongly stressed BLMs are higher than those observed for non-stressed BLM indicating a lower resistance for flow of current. These results imply that the stacking defects caused in BLMs due to oxidative stress can lead to an altered membrane physiology as a result of change in membrane permeability during oxidative stress, which is further investigated in the following sections. The stacking ability seems to be the maximum in the strongly stressed BLM, which had the lowest impedance values or the highest conducting ability. It is the minimum in the strongly stressed BLM, which had the highest impedance values or the lowest current conducting ability. These results are thus consistent with our previous results.

Accepted Manuscript

ACCEPTED MANUSCRIPT

The capacitance (C) reflects the charge storing ability of BLM across the two parallel plates, formed at BLM-bulk interface, and dielectric of BLM-capacitor is formed by hydrocarbon chains of well stacked lipids between two such plates. The capacitance is directly proportional to the membrane area, A_r, and inversely proportional to the BLM thickness, d, and is expressed as $C = \varepsilon_0\varepsilon_r (A_r d^{-1})$, where $\varepsilon_0\varepsilon_r$ is the relative permittivity of the dielectric formed by hydrocarbon chains of lipids [29] (Figure 2a). As the voltage is increased across BLM, more ions form the bulk approach zwitter-ionic polar heads at the BLM-bulk interface. This continuous increase of ionic pressure on ultra thin bilayer causes a strain to BLM that leads to decrease in d or/and increase in A_r and net result is increased C [30].

. In a voltage dispersion study, the BLM capacitance was found to increase with increasing AC voltage (Figure 2b). The BLM capacitance at 40 mV for non-stressed, mildly and strongly stressed samples was observed to be 0.34 nF, 0.85 nF, and 1.45 nF, respectively. With a further step increase in voltage, there was a gradual increase in capacitance of all the three types of BLMs. At 150 mV, the non-stressed BLM C value increased to 0.4 nF. The mildly and the strongly stressed BLMs, however, showed a higher increase in C with values reaching, 1.22 nF and 2.28 nF respectively.

The increased C in the strongly stressed BLM can be due to two reasons. One, the addition of oxidized functional group due to lipid peroxidation of UFA changes the conformation of lipid, such that the oxidized tails bend towards the aqueous phase [31]. Exposure of such polar groups in oxidized lipids to ions present in the aqueous phase leads to increased charge (Q) binding ability of the BLM-capacitor (Q increase in $C = QV^{-1}$). The second reason for the increase in C could be a high ionic pressure caused due

Accepted Manuscript

ACCEPTED MANUSCRIPT

to increased ionic interaction with oxidized functional groups further compress the BLM causing its thinning. A decrease in the thickness of membrane (decreased d in $C = \varepsilon_0\varepsilon_r (A_r d^{-1})$) results in increased C values (Figure 2a). Similar conclusions are also obtained from the values of capacitance calculated from charge-discharge study of BLM (Table 1).

The hydrocarbon chains of the bilayer, which form the dielectric of the BLM-capacitor, are in continuous vibratory motion, and an increase in voltage creates deformities in the BLM leading to its breakdown [32]. The mildly and strongly stressed BLM showed a lower breakdown voltage of 150 mV and 160 mV respectively compared to 250 mV for the non-stressed BLM (Figure 2b). Since an increase in the hydrocarbon chain symmetry leads to better packing, and hence higher breakdown voltages, the results indicate a more symmetrical packing of lipids with lesser defects in non-stressed BLM as compared to mildly and strongly stressed BLM.

The changes observed in the four electrical parameters (θ, Z, C and break down voltage) in our work, support the simulation results published earlier [31, 33-36], and reiterate that non-stressed BLM has a more robust arrangement in which the lipids are well stacked as compared to stressed BLM. For example, molecular dynamics (MD) studies performed on phosphatidylcholine (PC) and sphingomyelin (SM) bilayers, with varying double bond position on hydrocarbon chain, suggested that lipids with saturated acyl chains are more tightly packed than their mono-unsaturated counterparts [34, 35]. Introduction of unsaturated chain increased the fluidity and decreased the packing density of lipids in the zone of unsaturation. An oxidizing free radical passing through this zone will have higher solubility in this zone than in the saturated area close to the polar heads. This increased disorder may increase the reactivity of hydroxyl radical with UFA, leading

ACCEPTED MANUSCRIPT

to lipid peroxidation [33]. Computer simulations, assuming a homogeneous or heterogeneous membrane composition, have also predicted that the lipids damaged due to peroxidation modify the organization of biological membrane [36] and can make the membrane more permeable due to the presence of oxidized lipids [31].

Thus, both the phenomena i.e. increased UFA fraction with unsaturated chains in the bilayer and lipid peroxidation of these UFA, which contribute to the increased deformity in bilayer membrane, are expected to occur in *B. subtilis* cell during oxidative stress.

Oxidative stress increases lipid peroxidation

Lipid peroxidation has been known to occur when hydroxyl radical attacks the unsaturated lipids in cellular membranes [21]. The hydroxyl radical has a short half life of 10^{-9} s [37] and the lipid peroxidation rate constant is 5 X 10^{8} $M^{-1}s^{-1}$. Therefore, the hydroxyl radical quickly reacts with UFA leading to irreversible membrane damage [38]. The UFA in the cell membranes are oxidized to lipid peroxides, which in turn, are decomposed to carbonyl compounds such as malondialdehyde (MDA), which can be quantified using thiobarbituric acid (TBA assay), and used as a measure of lipid peroxidation. The MDA formed can be present along with the isolated lipids as well as with the proteins in the supernatant (protein "bound" MDA) [21].

The results of the TBA assay presented in Figure 3a shows a 59% increase and a 246% increase in MDA under mild and strong stresses, respectively, compared to the control, for the lipid fraction. Similarly, a 7% and 124% increase in MDA under mild and strong stresses, respectively, compared to the control, was observed in the supernatant (Figure 3b). Since MDA is the byproduct of lipid peroxidation by hydroxyl

ACCEPTED MANUSCRIPT

radicals, which results in the shortening of fatty acid chain length at points of unsaturation, the results indicate the extent of loss of UFA chain segments in the lipid bilayer. The chain segment loss leads to generation of two hydrocarbon chains of different length on the affected lipid. When these lipids are packed into a bilayer membrane (BLM) the membrane asymmetry is higher compared to a BLM comprised of non-damaged lipids [39]. The voids created due to inefficient packing of such peroxidized lipids can allow diffusion of smaller molecules or ions through them [27, 40].

Further, lipid peroxidation is expected to lead to a decrease in the UFA fraction since UFA is a substrate for the hydroxyl radical during lipid peroxidation. But, interestingly, we observed a net increase as described in the next section.

Oxidative stress increases UFA fraction

The increased MDA formation shown in the previous section indicated that the UFA fraction in the membrane that is expected to decrease under oxidative stress, may have actually increased. The extent of unsaturation or the fraction of UFA in the membrane lipids can be determined by measuring the Iodine number [22] using the lipids isolated from non-stressed, mildly stressed and strongly stressed samples. The results given in Figure 4 show that there was a 42.8% and 127% increase in unsaturation in mildly and strongly stressed cultures, respectively as compared to non stressed culture.

From the above results we have estimated the UFA present in the form of phospholipid in *B. subtilis* cell membrane, during non-stressed and oxidative stress conditions as discussed below. Considering *B. subtilis* as a cylinder with length of 2 μm,

ACCEPTED MANUSCRIPT

diameter of 1 μm, with a specific gravity of 1.04 [41], the mass of a single cell is 1.63 X 10^{-9} mg. With the data on our lipid yield, 38.27 mg (g-cell)$^{-1}$, and as assumed efficiency of 80% for the lipid extraction, it is estimated that the total lipid content of a single *B. subtilis* cell is 78 X 10^{-15} g. Under non-stressed conditions, *B. subtilis* cell membrane contains nearly 3% UFA of the total lipids, and the UFA are present mostly in the form of phospholipids [19, 42], and thus it is estimated that 2.34 X 10^{-15} g of unsaturated phospholipids are present per cell. Since phosphatidylcholine is the one of the predominant species of phospholipids present in cell membranes [43], for the purposes of this estimation, let us assume that all UFA exist as phosphatidylcholine ($C_{42}H_{82}NO_8P$), UFA-PC, with a molecular weight of 760.09 g mol^{-1}. From the above, it is estimated that a single non-stressed cell contains 3.07 X 10^{-12} μmoles of UFA. A 42.8% over this value for mildly stressed lipid sample suggest that 4.38 X 10^{-12} μmoles UFA-PC is present per cell under mild oxidative stress. Similarly a 127% increase in iodine number suggests that 6.97 X10^{-12} μmoles UFA-PC is present per cell under strong oxidative stress. An increase in UFA has been reported when *B. subtilis* cells were subjected to cold stress [6].

To test the effect of UFA on the BLM stability, we performed experiments with a synthetic phospholipid, L-alpha-phosphatidylcholine (PC) and a known UFA, linoleic acid. We increased the percentage of linoleic acid in PC-BLM and the results have been summarized in Table 2. Decreases in the values of θ and breakdown voltage were observed with increases in the percentage of linoleic acid of the PC-BLM. These results strengthened our observation that decreases in the electrical parameters observed in strongly stressed BLM, may be due to increased UFA fraction in addition to damaged lipids caused by lipid peroxidation.

ACCEPTED MANUSCRIPT

It is known that the UFA are negative regulators for Δ5 acyl lipid desaturase, the enzyme needed to synthesize UFA [44, 45]. Therefore, a decrease in UFA due to MDA formation during lipid peroxidation during oxidative stress may activate Δ5 acyl lipid desaturase [46], which in turn, may lead to production of UFA, which in turn leads to an increase in the UFA fraction in the membrane. Thus the observed increase in membrane UFA fraction is most likely due to an increased synthesis of UFA under oxidative stress.

Electrical parameters of *B. subtilis* BLM

The electrical parameters of the *B. subtilis* BLM may be helpful in mathematical modeling and in electrophysiological studies involving *B. subtilis* membrane in particular, and prokaryotic cellular lipid membrane in general. Such parameters from DC voltage dispersion studies on *B. subtilis* BLM, which have not been reported earlier, are given in this section. For a BLM capacitor, current (I) and charge (Q) have been represented here by the equations (1 and 2). The equation 3 [25] gives the relationship between the charge, q, and the electromotive force (EMF), E for a standard capacitor.

$$I = A' X \exp^{\lambda t} + Leakage\ \ current \qquad (1)$$

$$Q = \frac{A'}{\lambda}(\exp^{\lambda t} - 1) \qquad (2)$$

$$q = EC(1 - e^{t/RC}) \qquad (3)$$

The term, $A'\lambda^{-1}$, for the BLM capacitor is equivalent to EC (maximum charge stored in capacitor) for a standard capacitor, and λ of the BLM capacitor is equivalent to $-(RC)^{-1}$ (where R is the total resistance and RC is the time constant (τ) of circuit) of the standard capacitor. To determine the values of parameters such as A', λ, τ, leakage current, DC

ACCEPTED MANUSCRIPT

capacitance and relative permittivity, we studied the charging and discharging behavior of BLM capacitance at four different DC voltages. One such cycle of charging and discharging of BLM-capacitor at 40 mV has been shown in Figure 5. All the parameters were determined using MATLAB, from the data accumulated during study of charging and discharging patterns of all three types of BLM at four different voltages. The values of these parameters have been summarized in Table 1.

Time constant, tau ($\tau = RC$) of the capacitor (Table 1) is defined as time required by the charge on capacitor to reach 63% of its final steady state value EC (taken at 6.63 s in this study). We have considered the resistance of BLM as negligible (few hundreds Kohm) in comparison to 1 Gohm resistor used in the circuit in all our calculations. The leakage current was also observed to increase with increasing DC voltage, and the increase was more in the strongly stressed BLM compared to the mildly stressed and non-stressed BLM. The relative permittivity constants, $\varepsilon_0\varepsilon_r$ of non-stressed, mildly and strongly stressed BLM were estimated with two assumptions, i.e. (i) Effective BLM area is 60% of aperture area (0.00705 cm^2) [47] (ii) Thickness of BLM was assumed to be 50Å irrespective of applied voltage. [30]. The $\varepsilon_0\varepsilon_r$ value of non-stressed, mildly and strongly stressed BLM were found to be $1.03X10^{-11}$, $1.15\ X10^{-11}$ and $1.34\ X10^{-11}$ Fm^{-1} respectively. These estimated values were found to be of same magnitude to that of the *E. coli* BLM which was reported to be $4.4X10^{-11}$ Fm^{-1} [30].

Accepted Manuscript

ACCEPTED MANUSCRIPT

Increased membrane permeability: A strategy to improve specific protein productivity

The changed membrane physiology in *B. subtilis* reported in this study, due to increased cell membrane permeability under oxidative stress conditions can possibly be used to improve specific protein productivity. An increased permeability caused by lipid peroxidation and increased UFA fraction, is expected to disrupt ion gradients leading to altered metabolic processes [31, 34]. The increased membrane permeability in strongly stressed BLM, is expected to allow H_2O_2 diffusion at higher rates, leading to higher intracellular H_2O_2 concentrations [48, 49], and thus increased oxidative stress. The specific production of certain proteins, especially protective proteins, is known to be increased under oxidative stress in *B. subtilis* [49-51].

In this study, the specific productivity of two industrially important enzymes protease and amylase, showed significant increases of 61.6% and 136.7%, respectively, under strongly stressed condition compared to the non-stressed condition (Figure 6). In addition to increased diffusion rate of H_2O_2 inside the cell [48], which can induce higher protein expression rates [50], an increased secretion rate of extracellular proteins due to the higher permeability of the cell membrane may also be responsible for increased specific enzyme productivity in strongly stressed cells.

Accepted Manuscript

ACCEPTED MANUSCRIPT

Conclusions

The isolated lipids from non-stressed, mildly and strongly stressed *B. subtilis* lipids when reconstituted to form BLMs, showed marked differences in their electrical properties. Modifications in four electrical parameters such as phase angle, impedance, capacitance and breakdown voltage emphasized that the packing of lipids in non-stressed BLM was more compact than in mildly and strongly stressed BLMs. The increased permeability in strongly-stressed BLM as compared to non-stressed BLM was due to two phenomena occurring in *B. subtilis* during oxidative stress: (i) the damage to UFA by hydroxyl radical during lipid peroxidation (59% and 246% increase in MDA formation under mild and strong stresses, respectively), and the consequent loose packing of the damaged lipids in the reconstituted BLM (ii) an increase in the fraction of UFA in the membrane (42.8% and 127% increase in iodine number under mild and strong stresses, respectively), and the consequent increase in fluidity and decrease in the packing density of lipids. Important electrical parameters of the BLMs such as $A^{'}$, λ, τ, leakage current, DC capacitance and relative permittivity were determined in this study. Finally, we demonstrated that increased permeability during oxidative stress can be used as an effective strategy to increase the specific productivity of amylase and protease. These enzymes showed considerable increases of 61.6% and 136.7%, respectively, under strongly stressed condition compared to the non-stressed condition.

Acknowledgement

Vijesh Kumar, SASTRA University, is acknowledged for his help.

ACCEPTED MANUSCRIPT

List of symbols

$A^{'}$	Parameter of the BLM capacitor that equals $-(ER^{-1})$ of the standard capacitor (A)
A_r	Area of BLM (cm^2)
C	Capacitance (nF)
d	Thickness of BLM (Å)
E	Electromotive force (EMF) of the DC source (mV)
I	Current flowing through an AC/DC circuit (pA)
I_0	Maximum value of current in an AC circuit (pA)
Q	Charge stored in the BLM-capacitor (pC)
q	Charge stored in the standard capacitor (pC)
R	Total resistance of the DC circuit (Gohm)
t	Time (s)
V	Voltage (mV) across the AC circuit (mV)
V_0	Maximum voltage across AC circuit (mV)
Z	Impedance (Mohm)

Greek symbols

ε_0	Permittivity of free space (8.85×10^{-12} Fm^{-1})
ε_r	Relative permittivity (Fm^{-1})
λ	Parameter of the BLM capacitor that equals $-(RC)^{-1}$ of the standard capacitor (s^{-1})
τ	Time constant, ($= RC$) (s)
θ	Phase lag between the V and I (^{o})
ω	Angular frequency (s^{-1})

Accepted Manuscript

ACCEPTED MANUSCRIPT

References

[1] Marrink SJ, Berendsen HJC, Permeation process of small molecules across lipid membranes studied by molecular dynamics simulations. J Phys Chem 1996;100:16729-16738.

[2] Lopez SC, Heras H, Ruzzal SM, Sánchez-Rivas C, Rivas EA, Variations of the envelope composition of *Bacillus subtilis* during growth in hyperosmotic medium. Curr Microbiol 1998;36:55-61.

[3] Zhang YM, Rock CO, Membrane lipid homeostasis in bacteria. *Nat Rev Microbiol. 2008;6:222-233.*

[4] Mansilla MC, Banchio CE, de Mendoza D, Signalling pathways controlling fatty acid desaturation, *Subcell Biochem 2008;49:71-99.*

[5] Guerzoni ME, Lanciotti R, Cocconcelli PS, Alteration in cellular fatty acid composition as a response to salt, acid, oxidative and thermal stresses in *Lactobacillus helveticus*. Microbiology 2001; 147:2255–2264.

[6] Weber MHW, Klein W, Muller L, Niess UM, Marahiel MA, Role of the *Bacillus subtilis* fatty acid desaturase in membrane adaptation during cold shock. Mol Microbiol 2001; 39:1321-1329.

[7] Aguilar PS, Cronan Jr. JE, Mendoza DDA, *Bacillus subtilis* gene induced by cold shock encodes a membrane phospholipid desaturase. J Bacteriol 1998;180:2194–2200.

[8] Hancock JT, Desikan R, Neill SJ, Role of reactive oxygen species in cell signalling pathways. Biochem Soc Transact 2001; 29:345-350.

Accepted Manuscript

ACCEPTED MANUSCRIPT

[9] Mishra S, Noronha SB, Suraishkumar GK, Increase in enzyme productivity by induced oxidative stress in *Bacillus subtilis* cultures and analysis of its mechanism using microarray data. Process Biochem 2005; 40:1863-1870.

[10] Henle ES, Luo Y, Gassman W, Linn S, Oxidative damage to DNA constituents by iron-mediated fenton reactions: the deoxyguanosine family. J Biol Chem 1996; 271:21177-21186.

[11] Antunes F, Cadenas E, Estimation of H_2O_2 gradients across biomembranes. FEBS Lett 2000; 475:121-126.

[12] Makino N, Sasaki K, Hashida K, Sakakura YA, Metabolic model describing the H_2O_2 elimination by mammalian cells including H_2O_2 permeation through cytoplasmic and peroxisomal membranes: comparison with experimental data. Biochim Biophys Acta 2004;1673:149–159.

[13] Cabiscol E, Tamarit J, Ros J, Oxidative stress in bacteria and protein damage by reactive oxygen species. Internatl Microbiol 2000;3:3–8.

[14] Mostertz J, Hecker M, Patterns of protein carbonylation following oxidative stress in wild-type and sigB *Bacillus subtilis* cells. Mol Gen Genomics 2003;269:640–648.

[15] Hodges DM, DeLong JM, Forney CF, Prange RK, Improving the thiobarbituric acid-reactive-substances assay for estimating lipid peroxidation in plant tissue containing anthocyanins and other interfering compounds. Planta 1999;207:604-611.

[16] Köper I, Schiller SM, Giess F, Naumann R, Knoll W, Functional tethered bimolecular membranes (tBLMs). In: Liu LA, Leitmannova AO, Tien HT, editors, Advances in Planar Lipid Bilayers and Liposomes. vol. 3. New York: Academic Press; 2006. p. 37-40.

Accepted Manuscript

ACCEPTED MANUSCRIPT

[17] Tien HT, Bilayer lipid membrane theory and practice. New York: Marcel Dekker Inc.; 1974. p. 655

[18] Bligh EG, Dyer WJA, Rapid method of total lipid extraction and purification. Can J Biochem Physiol 1959;8:911–917.

[19] Kaneda T, Fatty acids of the genus *Bacillus*: An example of branched chain preference. Bacteriol Rev 1977;41:391-418.

[20] Antczak A, Nowak D, Shariati B, Król M, Piasecka G, Kurmanowska Z, Increased hydrogen peroxide and thiobarbituric acid-reactive products in expired breath condensate of asthmatic patients. Eur Respir J 1997;10:1235–1241.

[21] Garcia YJ, Rodríguez-Malaver AJ, Peñaloza N, Lipid peroxidation measurement by thiobarbituric acid assay in rat cerebellar slices. J Neurosci Methods 2005;144:127–135.

[22] Yasuda M. The determination of the iodine number of lipids. J Biol Chem 1931;94:401-409.

[23] Rajagopalan G, Krishnan C, α-Amylase production from catabolite derepressed *Bacillus subtilis* KCC103 utilizing sugarcane bagasse hydrolysate. Bioresource Tech 2008;99:3044-3050.

[24] Tien HT, Ottova A. The bilayer lipid membrane (BLM) under electrical fields. IEEE Trans Dielec Electr Insul 2003;10:717-727.

[25] Palit S, Principles of electricity and magnetism. New Delhi: Narosa publishing house; 2005. p. 124.

[26] Carstensen EL, Marquis RE, Child SZ, Bender GR, Dielectric properties of native and decoated spores of - *Bacillus megaterium*. J Bacteriol 1979;140:917-928.

Accepted Manuscript

ACCEPTED MANUSCRIPT

[27] Hagge SO, Wiese A, Seydel U, Gutsmann T, Inner field compensation as a tool for the characterization of asymmetric membranes and peptide-membrane interactions. Biophys J 2004;86:913–922.

[28] Bordi F, Cametti C, Gliozzi A, Impedance measurements of self-assembled lipid bilayer membranes on the tip of an electrode. Bioelectrochemistry 2002;57:39-46.

[29] Islam N, Bulla NA, Islam S, Electrical double layer at the peritoneal membrane/electrolyte interface. J Membrane Sc 2006;282:89–95.

[30] Chalise PR, Perni S, Shama G, Novac BM, Smith IR, Konga MG, Lethality mechanisms in *Escherichia coli* induced by intense sub-microsecond electrical pulses. Appl Phys Lett 2006;89:1539021-1539023.

[31] Wong-ekkabut J, Xu Z, Triampo W, Tang IM, Tieleman DP, Monticell, L, Effect of lipid peroxidation on the properties of lipid bilayers: a molecular dynamics study. Biophys J 2007;93:4225–4236.

[32] Kramar P, Miklavcic D, Lebar AM, Determination of the lipid bilayer breakdown voltage by means of linear rising signal. Bioelectrochemistry 2007;70:23–27.

[33] Bachar M, Brunelle P, Tieleman DP, Rauk A, Molecular dynamics simulation of a polyunsaturated lipid bilayer susceptible to lipid peroxidation. J Phys Chem B 2004 ;108:7170-7179.

[34] Hyvönen MT, Kovanen PT, Molecular dynamics simulations of unsaturated lipid bilayers: effects of varying the numbers of double bonds. Eur Biophys J 2005;*34*:294–305.

[35] Niemelä PS, Hyvönen MT, Vattulainen I, Influence of chain length and unsaturation on sphingomyelin bilayers. Biophys J 2006;90:851–863.

Accepted Manuscript

ACCEPTED MANUSCRIPT

[36] Sabatini K, Mattila JP, Megli FM, Kinnunen PKJ, Characterization of two oxidatively modified phospholipids in mixed monolayers with DPPC. Biophys J 2006;90:4488–4499.

[37] Ghosh SK, Tapatichakraborti, Banerjee AB, Roychoudhury S, Chakrabortia S, Role of hydroxyl radical in superoxide induced microsomal lipid peroxidation: protective effect of anion channel blocker. J Biosci 1996;21:35-43.

[38] Storey KB, *Functional Metabolism: Regulation and Adaptation*. New York: Wiley-IEEE; 2005. p. 345.

[39] Diederich A, Bähr G, Winterhalter M, Influence of surface charges on the rupture of black lipid membranes. Phys Rev E 1998;58:4883-4889.

[40] Gallucci E, Micelli S, Monticelli G, Pore formation in lipid bilayer membranes made of phosphatidylinositol and oxidized cholesterol followed by means of alternating current. Biophys J 1996;71:824-831.

[41] Kendall I, Bacteriology - general, pathological and intestinal. New York: Fitts Press; 2007. p. 25.

[42] Bishop DG, Rutberga L, Samuelsson B, The chemical composition of the cytoplasmic membrane of *Bacillus subtilis.* European J Biochem 1967;2:448-453.

[43] Pomerantsev AP, Kalnin KV, Osorio M, Leppla SH, Phosphatidylcholine-specific phospholipase C and sphingomyelinase activities in bacteria of the *Bacillus cereus* group. Infect Immun 2003;71:6591–6606.

[44] Bonamorea A, Maconea A, Colotti G, Matarese RM, Boffia A, The desaturase from *Bacillus subtilis*, a promising tool for the selective olefination of phospholipids. J Bacteriol 2006;121:49–53.

Accepted Manuscript

ACCEPTED MANUSCRIPT

[45] Mansilla CM, Mendoza DD, The *Bacillus subtilis* desaturase: a model to understand phospholipid modification and temperature sensing. Arch Microbiol 2005;183:229–235.

[46] Altabe SG, Aguilar P, Caballer GM, Mendoza DD, The *Bacillus subtilis a*cyl lipid desaturase is a Δ5 Desaturase. J Bacteriol 2003;185:3228–3231.

[47] Bienert GP, Schjoerring JK, Jahn TP, Membrane transport of hydrogen peroxide. Biochim Biophys Acta 2006;1758:994–1003.

[48] Mathai JC, Sitaramam V, Stretch sensitivity of transmembrane mobility of hydrogen peroxide through voids in the bilayer. J Biol Chem 1994;269:17784-17793.

[49] Fuangthong M, Herbig AF, Bsat N, Helmann JD, Regulation of the *Bacillus subtilis fur* and *perR g*enes by PerR: not all members of the PerR regulon are peroxide inducible. J Bacteriol 2002;184:3276–3286.

[50] Hayashi K, Ohsawa T, Kobayashi K, Ogasawara N, Ogura M, The H_2O_2 stress-responsive regulator PerR positively regulates *srfA* expression in *Bacillus subtilis.* J Bacteriol 2005;187:6659–6667.

[51] Hecker M, Völker U, Non-specific, general and multiple stress resistance of growth-restricted *Bacillus subtilis* cells by the expression of the σ^B regulon. Mol Microbiol 1998;29:1129-1136.

ACCEPTED MANUSCRIPT

Tables

Table 1. Electrical parameters of non-stressed, mildly and strongly stressed BLMs at different applied DC voltages.

Source Voltage (mV)	Stress sample type	$A^{'}$ X 10^{-11} (A)	λ (s^{-1})	τ (s)	Leakage current (pA)	C (nF)
40	Non	2.24 ± 0.01	-1.23 ± 0.14	0.805 ± 0.09	6.36 ± 0.13	0.805 ± 0.09
	Mild	1.66 ± 0.14	-1.02 ± 0.06	0.968 ± 0.01	6.67 ± 0.05	0.968 ± 0.01
	Strong	3.96 ± 0.26	-0.88 ± 0.08	1.11 ± 0.13	32.15 ± 0.10	1.11 ± 0.13
70	Non	3.29 ± 0.20	-1.12 ± 0.01	0.828 ± 0.01	10.37 ± 0.02	0.828 ± 0.01
	Mild	2.36 ± 0.38	-1.03 ± 0.10	0.961 ± 0.09	10.05 ± 0.10	0.961 ± 0.09
	Strong	3.86 ± 0.03	-0.80 ± 0.13	1.24 ± 0.20	34.0 ± 0.64	1.242 ± 0.20
100	Non	4.04 ± 0.48	-1.02 ± 0.06	0.966 ± 0.05	14.69 ± 0.05	0.966 ± 0.05
	Mild	3.50 ± 0.08	-1.04 ± 0.01	0.946 ± 0.01	13.64 ± 0.01	0.946 ± 0.01
	Strong	5.32 ± 0.96	-0.89 ± 0.06	1.12 ± 0.07	37.08 ± 0.26	1.113 ± 0.07
150	Non	5.94 ± 0.97	-0.98 ± 0.07	1.01 ± 0.07	23.19 ± 0.21	1.01 ± 0.07
	Mild	5.12 ± 0.41	-0.98 ± 0.08	1.01 ± 0.086	20.28 ± 0.06	1.01 ± 0.086
	Strong	6.32 ± 0.10	-0.94 ± 0.08	1.05 ± 0.09	41.06 ± 0.18	1.05 ± 0.09

Accepted Manuscript

ACCEPTED MANUSCRIPT

Table 2. Changes in the phase angle, θ, and breakdown voltage with changes in the percentage of linoleic acid (unsaturation) in PC-BLM.

% linoleic acid in PC-BLM	**Phase angle (θ)**	**Break down voltage (mV)**
0	-88°	250
20	-82°	130
40	-78°	50

Accepted Manuscript

ACCEPTED MANUSCRIPT

List of figures

Figure 1. Voltage dispersion **(a)** and Frequency dispersion **(b)** analysis of BLM impedance at constant AC frequency of 100 Hz and voltage of 40 mV respectively. Non-stressed BLM: filled circle, mildly stressed BLM: open triangle and strongly stressed BLM: open squares.

Figure 2. (a) The BLM acts as a capacitor in the bath solution. The polar heads of the lipids on both sides of the BLM are zwitterionic and interact with ions of opposite charges present in the bath solution. The long hydrocarbon chains of lipids act as insulators (dielectric) between the two conducting plates and act as a capacitor **(b)** Voltage dispersion analysis of BLM capacitance at constant AC frequency of 100 Hz. Non-stressed BLM: filled circle, mildly stressed BLM: open triangle and strongly stressed BLM: open squares.

Figure 3. MDA formation was determined in **(a)** isolated lipids and **(b)** in culture supernatant (MDA bound to proteins). Non-stressed: white bar, mildly stressed: gray bar and strongly stressed: black bar. All the values are the mean and SD of at least three observations.

Figure 4. Iodine number in the three kinds of samples. Non-stressed: white bar, mildly stressed: gray bar and strongly stressed: black bar. All the values are the mean and SD of at least three observations.

Figure 5. Charging and discharging patterns in three kinds of BLM at 40 mV DC voltage was independently recorded and superimposed. Non-stressed BLM: filled circle, mildly stressed BLM: open triangle and strongly stressed BLM: open squares.

Accepted Manuscript

ACCEPTED MANUSCRIPT

Figure 6. Specific amylase **(a)** and protease **(b)** productivity (units (g cell)$^{-1}$) in the culture supernatant. Non-stressed: white bar, mildly stressed: gray bar and strongly stressed: black bar. All the values are the mean and SD of at least three observations.

Accepted Manuscript

ACCEPTED MANUSCRIPT

Figure 1a

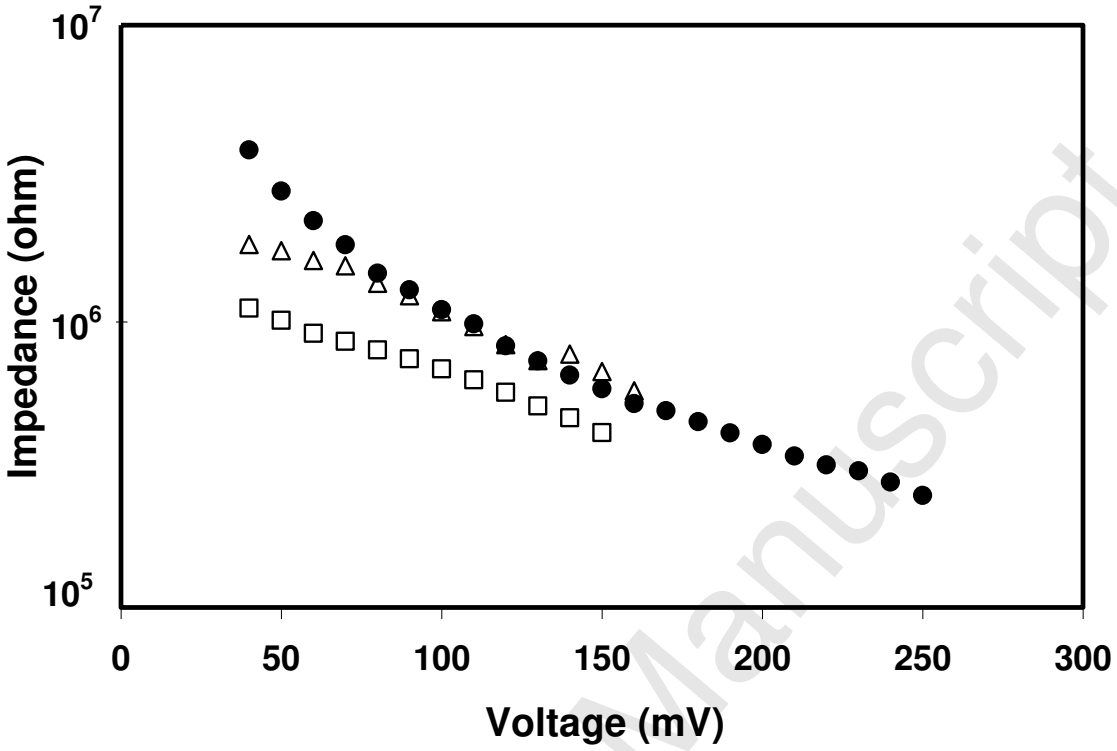

Figure 1b

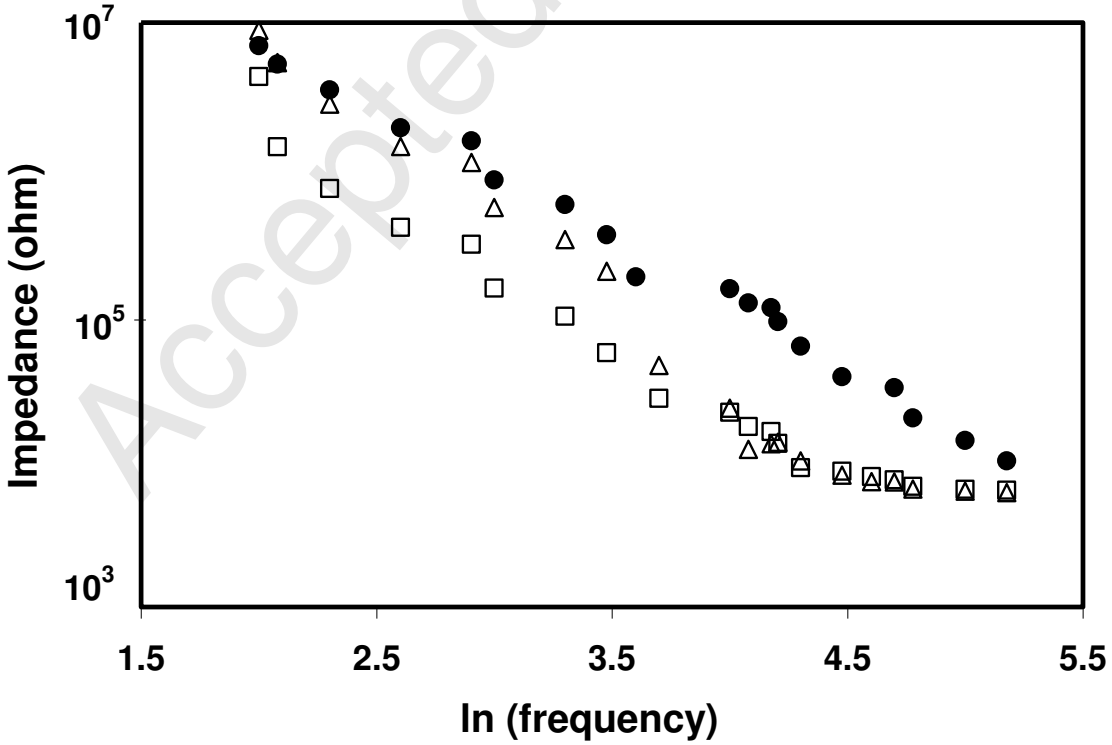

Accepted Manuscript

ACCEPTED MANUSCRIPT

Figure 2a

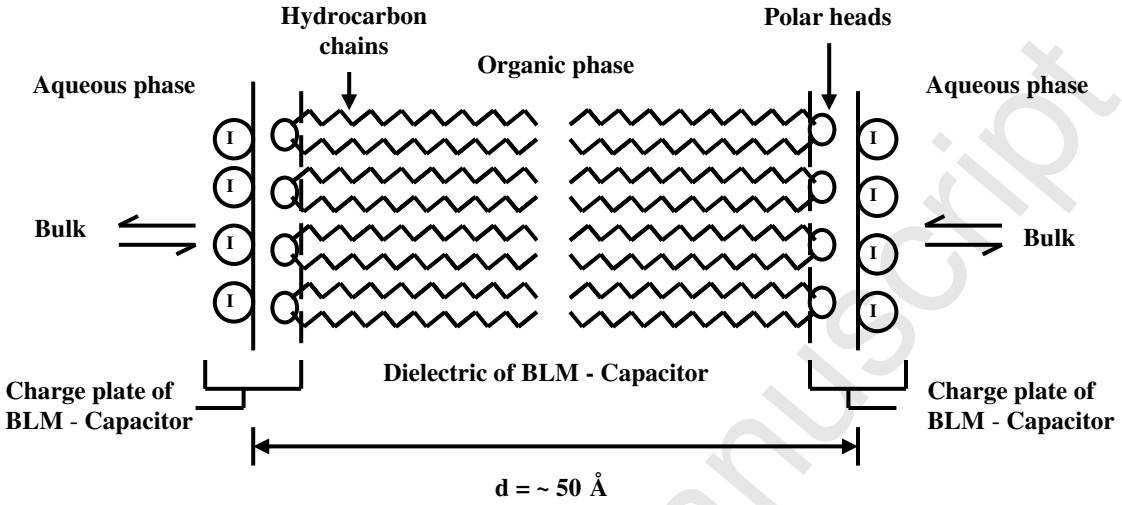

Figure 2b

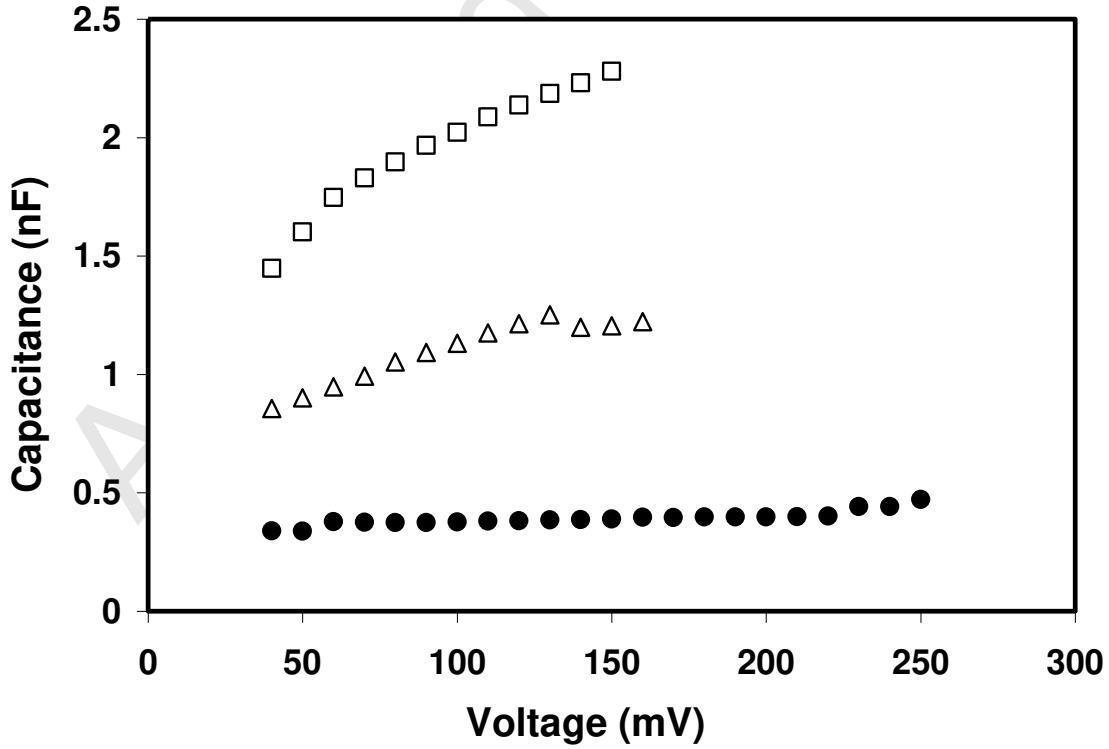

ACCEPTED MANUSCRIPT

Figure 3a

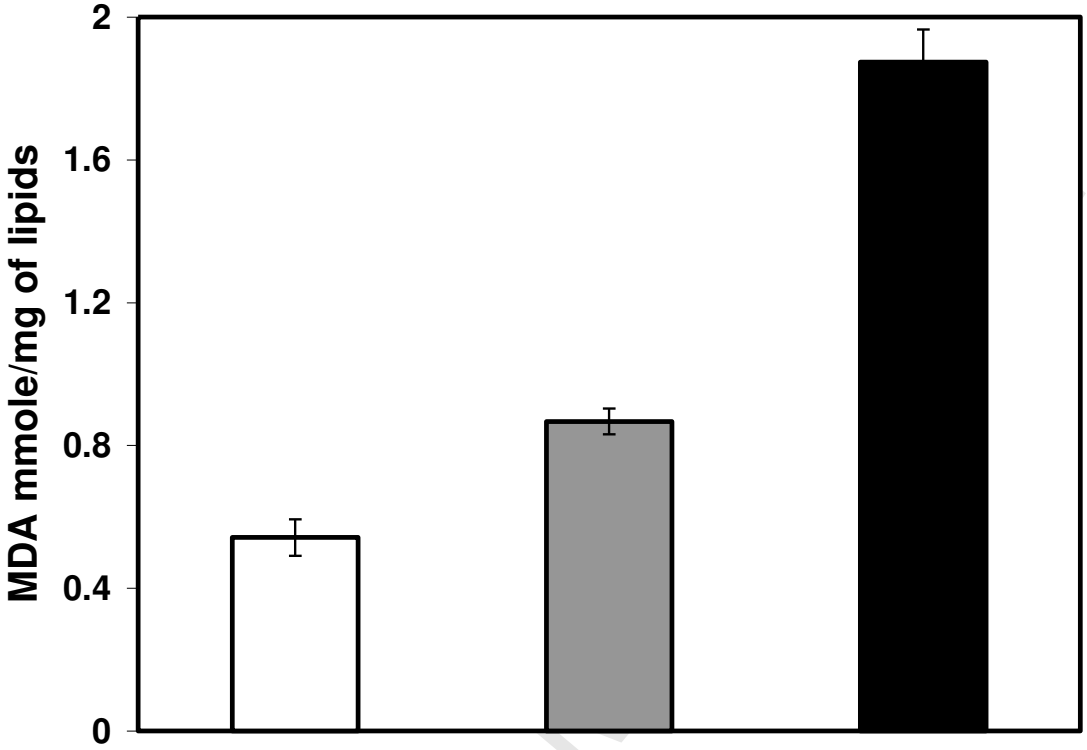

Figure 3b

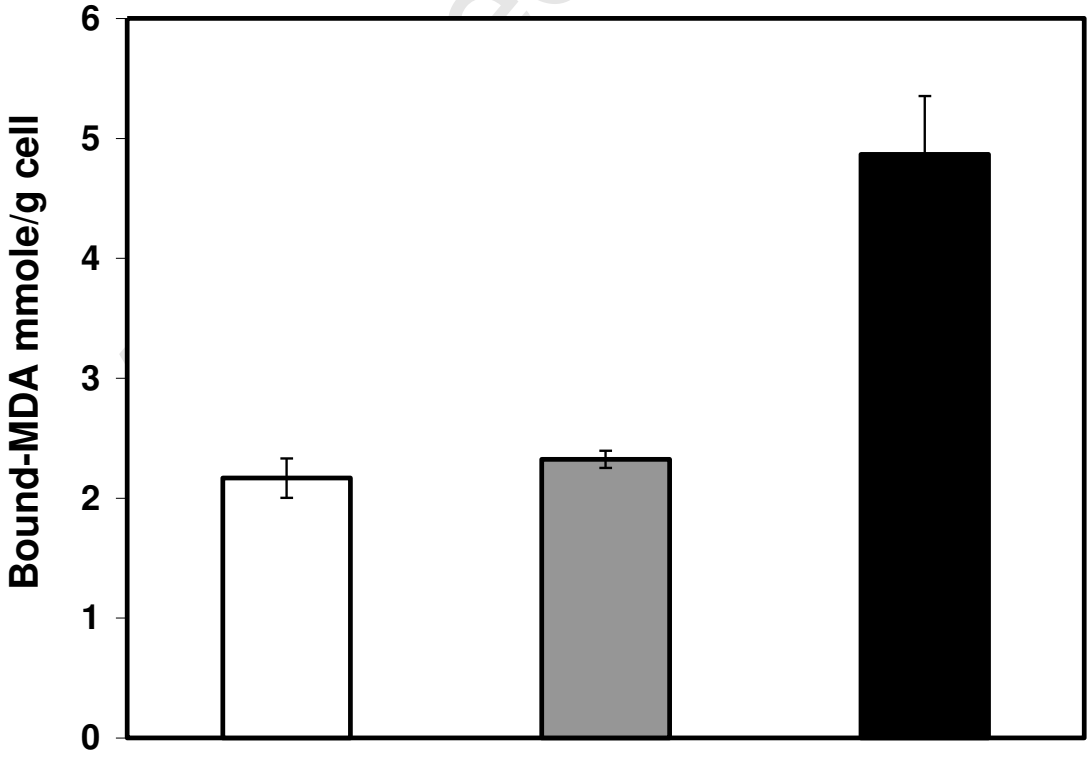

ACCEPTED MANUSCRIPT

Figure 4

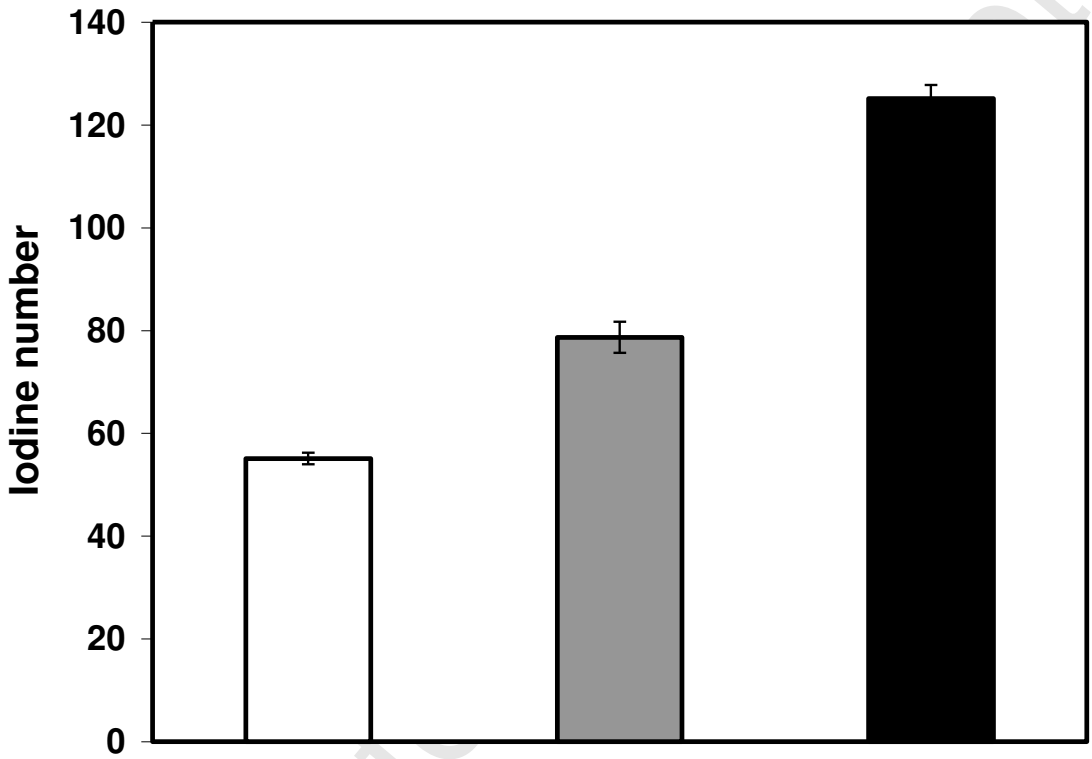

Accepted Manuscript

ACCEPTED MANUSCRIPT

Figure 5

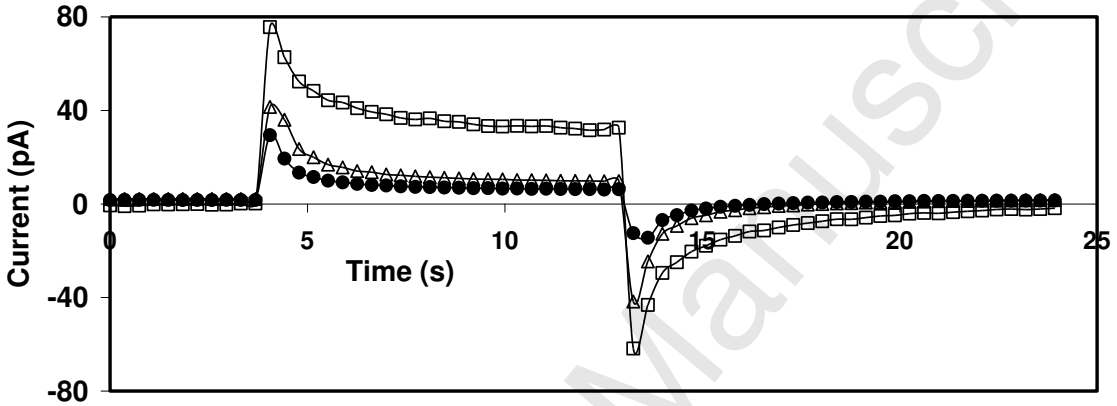

Accepted Manuscript

ACCEPTED MANUSCRIPT

Figure 6a

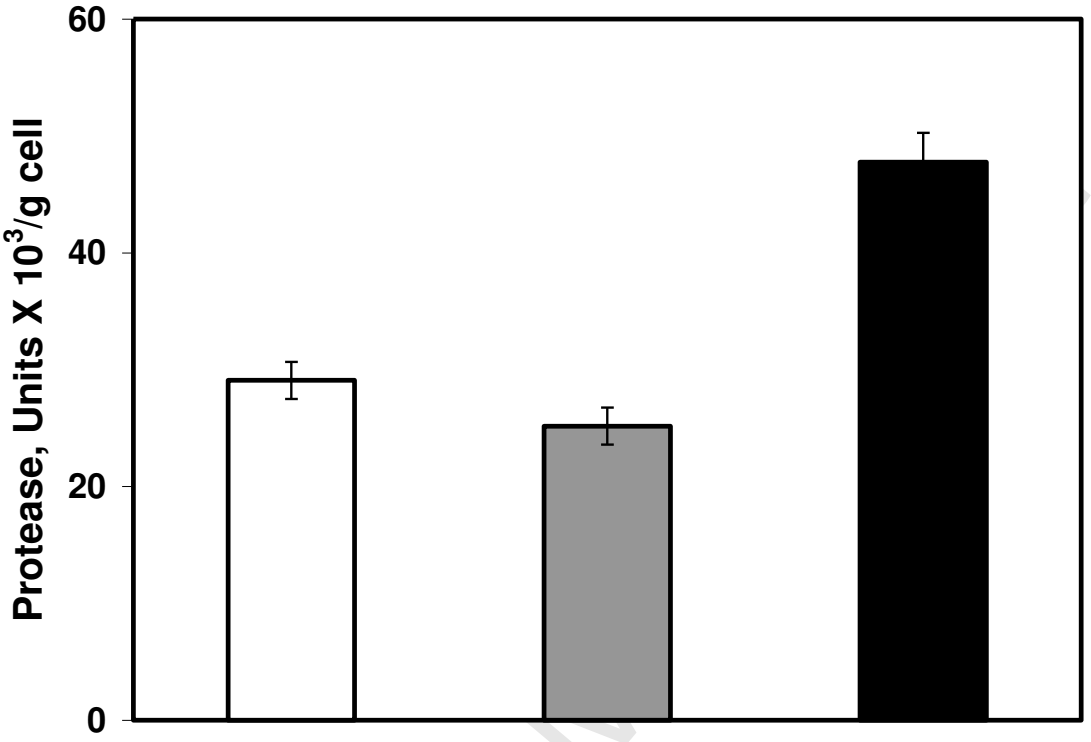

Figure 6b